COMPUTER METHODS AND PROGRAMS IN BIOMEDICINE 133 (2016) 45–54

journal homepage: www.intl.elsevierhealth.com/journals/cmpb

Using meta-differential evolution to enhance a calculation of a continuous blood glucose level

Tomas Koutny *

NTIS—New Technologies for the Information Society, Faculty of Applied Sciences, University of West Bohemia, Plzen 306 14, Czech Republic

ARTICLE INFO

Article history:
Received 7 January 2016
Received in revised form
11 April 2016
Accepted 23 May 2016

Keywords:
Continuous glucose monitoring
Glucose modeling
Blood glucose
Interstitial fluid
Differential evolution

ABSTRACT

We developed a new model of glucose dynamics. The model calculates blood glucose level as a function of transcapillary glucose transport. In previous studies, we validated the model with animal experiments. We used analytical method to determine model parameters. In this study, we validate the model with subjects with type 1 diabetes. In addition, we combine the analytic method with meta-differential evolution. To validate the model with human patients, we obtained a data set of type 1 diabetes study that was coordinated by Jaeb Center for Health Research. We calculated a continuous blood glucose level from continuously measured interstitial fluid glucose level. We used 6 different scenarios to ensure robust validation of the calculation. Over 96% of calculated blood glucose levels fit A+B zones of the Clarke Error Grid. No data set required any correction of model parameters during the time course of measuring. We successfully verified the possibility of calculating a continuous blood glucose level of subjects with type 1 diabetes. This study signals a successful transition of our research from an animal experiment to a human patient. Researchers can test our model with their data on-line at https://diabetes.zcu.cz.

1. Introduction

Glucose is primarily distributed in the blood through which it is transported across capillary membrane into the interstitial fluid of subcutaneous tissue [1,2]. In subcutaneous tissue, the interstitial fluid glucose level (IG) can be monitored continuously with a sensor of continuous glucose monitoring system (CGMS). The sensor comprises a needle that measures electrical current produced by glucose oxidase reaction in the subcutaneous tissue [3–5]. This current is mathematically filtered and wirelessly sent to the CGMS receiver, where it is converted to glucose level unit and downloaded to a computer [4,5]. Downloaded data comprise time series of IG with 5 minute interval between each two levels.

There is an immune response as the CGMS sensor is a foreign body [3,6]. Because of physiological interference, manufacturing tolerances and imperfections, the sensor must be repeatedly calibrated using blood glucose level (BG) [3–5]. To avoid calibration errors, IG should be steady so that it could be assumed that BG is steady as well and thus both levels agree. As sensor's precision degrades continually, despite the calibration procedure, the sensor must be replaced eventually.

Using a finger-stick, the patient draws a drop of capillary blood onto a test strip [7]. Then, a glucometer applies an electric voltage on the terminals of the strip so that an electric

* NTIS—New Technologies for the Information Society, Faculty of Applied Sciences, University of West Bohemia, Plzen 306 14, Czech Republic. Tel.: +420 377 632 437; fax: +420 377 632 401.
E-mail address: txkoutny@kiv.zcu.cz.

http://dx.doi.org/10.1016/j.cmpb.2016.05.011

current flows through the strip. This electric current is quantified, scaled and reported as glucose level [7].

Using a finger-stick, BG can only be monitored sporadically to avoid increasing the discomfort of the patient [8]. Minder et al. [9] pin-pointed 3 and 4 self-monitored blood glucose (SMBG) measurements a day. Petry et al. [10] reported SMBG increase from 2 to 5 measurements a day, if the patients earned monetary reinforcers. Beck et al. [11] explicitly state this: "requiring patients to do 6–8 SMBG a day at specified intervals for long periods of time will be too burdensome for most patients, and compliance with frequent middle-of-the-night measurements is likely to be low".

When self-measuring the blood glucose level, the patient could introduce an error as he could assign a wrong time to measured BG. Olansky and Kennedy [12] further reviewed the SMBG accuracy. In addition, Del Favero et al. [13] discussed human errors, erroneous data entry, and incorrect blood sampling/processing in the section on data pre-processing.

Inpatient closed-loop studies rely on BG measurements [11]. While CGMS solves the problem of sporadic BG measurements, it does not replace them. CGMS does not measure nor calculate BG. With outpatient studies, feasibility of SMBG is limited too [11]. Frequent and accurate reference BG is key for modeling and computing outcome metrics in clinical trials, but it is difficult, invasive, and costly to collect [13]. Continuous glucose monitoring (CGM) is a minimally-invasive technology that has the requested temporal resolution to substitute BG references for such a scope, but still lacks of precision and accuracy [13]. Therefore, we are motivated to calculate continuous BG from continuously measured IG. In this study, we validate our model of continuous BG calculation with subjects with type 1 diabetes. In addition, we present an extension to the original analytic method to determine model parameters.

1.1. *Related work*

Before we conducted this study, we considered other models of glucose dynamics. Only SMBG and CGMS are available in outpatient study. Therefore, we had to exclude models, which required additional measured quantities (e.g. insulin [14], rate of oxygen consumption [15,16], [18F]fluorodeoxglucose tracer [17]), from the consideration. Then, we excluded models which capture no physiological knowledge—e.g. Volterra–Wiener framework [18] and autoregressive model [19].

To the best of our knowledge, only the Steil–Rebrin model meets the required criteria. Equation (1) denotes this model; $b(t)$ and $i(t)$ symbols denote BG and IG respectively at time t.

$$\frac{\tau}{g}\times\frac{di(t)}{dt}+\frac{1}{g}\times i(t)=b(t) \tag{1}$$

Accordingly to References [20, 21], the g-parameter is steady-state gain and the τ-parameter is IG equilibration time constant. Considering steady state with no change of IG, the g-parameter should equal 1 as there would be zero concentration gradient between IG and BG. Nevertheless, estimating both parameters improves precision of the model [20,22].

Recently, Del Favero et al. [13] considered the g-parameter as 1 while adding a calibration-error model to restore a "true" IG, $i_t(t)$, using Equation (2). The α, β, and γ parameters are considered as calibration parameters, which must be re-determined whenever the CGMS sensor is calibrated. $\Delta t(t)$ is the time difference with respect to the last calibration time – t_{cal}.

$$i_t(t)=\frac{i(t)-\beta-\gamma\times\Delta t(t)}{\alpha};\quad \Delta t(t)=t-t_{cal} \tag{2}$$

From Equation (1), by substituting $i(t)$ with $i_t(t)$ of Equation (2), we obtain Equation (3). In Equation (3), $i(t)$ represents CGMS measured IG.

$$\frac{\tau}{g}\times\frac{\frac{di(t)}{dt}-\gamma}{\alpha}+\frac{1}{g}\times\frac{i(t)-\beta-\gamma\times\Delta t}{\infty}=b(t) \tag{3}$$

As Del Favero et al. [13] considered $g=1$, the α-parameter overtook the role of the g-parameter in Equation (1). Hence, we obtain Equation (4) that shows that Del Favero et al. [13] actually improve precision of the Steil–Rebrin model by adding simple linear regression with time as the explanatory variable. This variable is supposed to capture CGMS sensor degradation since last calibration. Therefore, α, β, and γ must be re-calculated with each calibration.

$$\frac{\tau}{\alpha}\times\frac{di(t)}{dt}+\frac{1}{\alpha}\times i(t)=b(t)+\left[\frac{\gamma}{\alpha}\times\Delta t(t)+\frac{\beta+\tau\times\gamma}{\alpha}\right] \tag{4}$$

Reference [8] queried diabetic type-1 patients' wishes and expectations on artificial pancreas. The patients asked for, i.a., minimal patient intervention, low maintenance, and ease of use. Therefore, we do not expect the patient to collect more BGs than those BGs that are required to keep CGMS calibrated, especially if these additional BGs would be used to re-determine model parameters until the next calibration only. Instead, we are going to meet patients' wishes by designing such a model whose parameters hold over several calibrations, possibly over the entire lifetime of the sensor.

2. Materials and methods

We developed a model that calculates BG from IG [22–25]. The model is based on a system of glucose dynamics and relates present BG and IG to future IG. We devised the physiological foundation of this model in Koutny [23]. Then, we further elaborated this physiological foundation in Koutny [24], where we have shown that model parameters correlate with glucose uptake rates of subcutaneous, skeletal muscle and visceral fat tissues. These rates correspond with other studies, which were conducted using different methods and experimental setups.

Fig. 1 depicts glucose flow in a selected part of glucose dynamics that is directly related to the model. Glucose may appear in the blood, e.g., due to consumed carbohydrates, the breakdown of liver glycogen or an infusion. From the blood, glucose is transported across the capillary membrane into the interstitial fluid. The rate of such a transport is limited by the size of capillary membrane surface, membrane permeability and concentration gradient between BG and IG [2]. In addition, this causes a delay in transport of glucose from blood into interstitial fluid. In the interstitial fluid, the glucose is either utilized

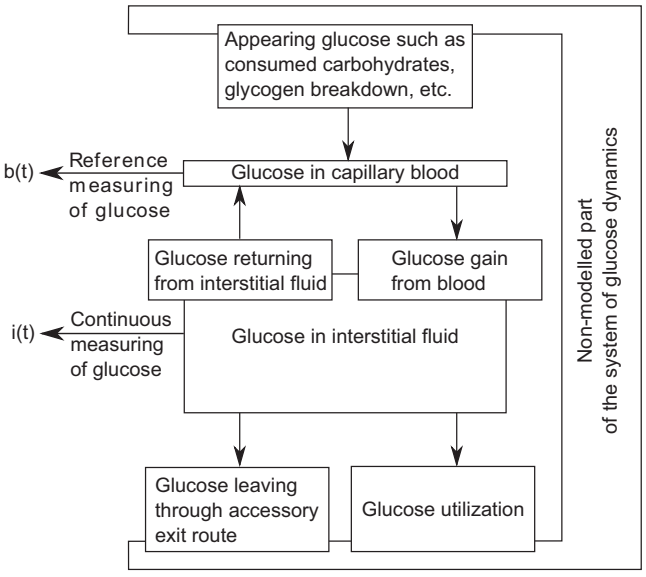

Fig. 1 – Block schema of glucose flow in a selected part of glucose dynamics.

or leaves the fluid. Depending on BG, part of IG can be transported back into the blood, with the same limits applied to the transport in the opposite direction. In addition, yet another part of IG can leave through an accessory exit route such as the lymphatic system, eventually appearing in the blood [1,2].

Both BG and IG affect each other. In addition, they are both controlled by a number of hormones, neural signals and substrate effects [1]. This is a complex system whose modeling would lead to a complex model with a considerable number of parameters. Such a model may be prone to overfitting. In such a case, the model would describe the error noise instead of capturing the relationship between the individual compartments of the system. In addition, too many parameters may make it impossible to identify if we do not have enough input levels to capture the dynamics of the glucose system.

Instead of designing a complex model, we approach the problem with an inspiration by federative co-simulation. In co-simulation, the entire system is decoupled into smaller parts, each of which is modeled with its own simulator. These simulators communicate with each other, while treating each other as a black box. In federative co-simulation such as high-level architecture, a simulator can be used together with a live device to increase the overall precision of entire simulation [26]. Our model describes the correlation between BG and IG across the capillary membrane. The blood and interstitial fluid represent interfaces that connect our model (simulator) to other compartments (devices) in the system. As a result, we do not need to calculate with other substances such as insulin that moderates the glucose uptake by cells. Instead of such a calculation, the biological system itself carries out the necessary actions and applies the results to BG and IG, which we read subsequently—thus having the effects of insulin already and precisely processed. As a result, the model requires no inputs such as insulin dosage or volume of consumed carbohydrates. The model requires only the continuous measuring of IG and several samples of BG to estimate model parameters by building an over-determined system of model equations. BG can be measured using either SMBG or a catheterized vein.

The model can run in parallel with the real transport of glucose across the capillary membrane. The model states that the glucose system changes IG in such a manner so that IG at three different times infers BG at one of those times. At the very beginning, we use BG to determine parameters of the model—i.e., quantifying the effects that exert an influence over the glucose transport across the capillary membrane. Then, we continuously measure IG to retrospectively calculate continuous BG. We compare calculated BG to measured BG to estimate the calculation error—see the metric in Section 2.2. Measured BG can be further used to calibrate CGMS, or to re-determine model parameters as needed.

In References [22–24], we derived Equations (5) and (6), i.e., the model used in this study, and described its parameters. According to these studies, the p-parameter is an arbitrary constant representing glucose gain from the blood across the capillary membrane. The cg-parameter is an arbitrary constant expressing the effect of the membrane surface area and permeability. $b(t) - i(t)$ is the concentration difference across the membrane according to Fick's Law of Diffusion [27]. The c-parameter is an arbitrary glucose level that represents the difference between the glucose appearance in the subcutaneous tissue and its clearance. Equation (5), i.e., $\varphi(t)$, is a time-varying offset of IG changes. It comprises a fixed part, the Δt-parameter, and a variable part, the h and k parameters. t is time since some fixed date. In our implementation, it is number of days since January 0, 1900 00:00 UTC; fractional part stores time of the day. The h-parameter has the same unit as Δt-parameter and t. The h-parameter gives an offset into the past from the time t. For an h-long interval, the k-parameter expresses the effect of the concentration gradient change rate as it affects the IG over this interval. It converts IG-observed change into a variable time-distance that is needed to obtain three IGs that infer single BG. For marginal values of IG time series, Equation (5) can produce such a time for which there is no measured IG. Then, BG cannot be calculated. As the time segment lasts for several days, it is negligible.

$$\varphi(t) = t + \Delta t + \begin{cases} k \times \dfrac{i(t) - i(t-h)}{h} & h \neq 0 \\ 0 & h = 0 \end{cases} \tag{5}$$

$$p \times b(t) + cg \times b(t) \times [b(t) - i(t)] + c = i(\varphi(t)) \tag{6}$$

2.1. Comparison with the Steil–Rebrin model

First, the Steil–Rebrin model calculates with a derivative of continuous function $i(t)$. Nevertheless, CGMS provides discrete time series so that we would have to either calculate numeric derivative in discrete time or derive a function that may differ from real $i(t)$. Therefore, we calculate with $b(t) - i(t)$ to express the difference between glucose levels on both sides of capillary membrane. In addition, it equals the first derivative of $i(t)$ according to the Steil–Rebrin model. Nevertheless, unit of τ is second, while unit of cg is [L/mmol]. Perhaps, the cg-parameter accommodates a factor of slowness (inverse velocity) of BG–IG equilibration.

Second, time lag of glucose transport from the vascular to interstitial space is an important factor. Basu et al. [28] observed a median time lag of 6.8 (4.8–9.8) minutes after an intravenous bolus of glucose isotopes. Basu et al. [28] collected data from six subjects with type 1 diabetes. Ward et al. [29] examined CGMS sensor time lag with respect to rising and falling glucose levels. Using a regression delay method, 8.9 (6.1–11.6) and 1.5 (2.6–5.5) minutes were determined for the rising and falling glucose levels, respectively. While the τ-parameter is a time-constant, the Steil–Rebrin model does not explicitly calculate with the time lag. We do so with Equation (5).

Third, once we explicitly calculate with the time-lag, we have to consider a residual mass of IG that is already present in the future interstitial fluid. While we do so with the c-parameter [24], the Steil–Rebrin model adds $\tau \times i'(t)$.

Fourth, Del Favero et al. [13] adds the error-calibration model of CGMS in the form simple linear regression. We agree that absolute difference between measured and calculated BG increases with time. We de-facto already implemented the Steil–Rebrin model with second order derivative [30] as suggested by Rebrin et al. [21], and tried to construct a BG-adjusting curve. To confirm assumptions of Del Favero et al. [13], the curve would have to be monotonic. But there was only one monotonic curve of all experiments. Therefore, we rather consider parameters of our model to be time-invariant. As a respective ISO standard requires the CGMS to exhibit a particular minimum accuracy, we chose not to duplicate respective efforts of CGMS engineers within our model.

Nevertheless, if we would consider linear regression to correct measured IG to obtain true IG, with measured IG as the explanatory variable, then Equations (5) and (6) would retain the same number and placement of their present parameters. Therefore, we must consider that parameters of these equations may correct calibration errors.

We already compared our model with the Steil–Rebrin model (that is the sensor model of Del Favero et al. [13]), and our model performed considerably better [22]. The comparison was done using frequent measuring of BG and IG with well calibrated sensors. With this comparison, the α, β and γ parameters were 1.0, 0.0 and 0.0 respectively. It was an animal, hyperglycemic clamp study.

To test their method with human patients, Del Favero et al. [12] used a well-selected glucose profile. For instance, a rate of change larger than 0.278 mmol/(L × min), or any values outside the range [2.222, 22.222] mmol/L, were considered suspicious and isolated [13]. In addition, they pre-processed the glucose series to detect and eliminate BG outliers. We do not do this. We rather take the measured levels "as-is", because the self-measured BG will be sparse in the practice.

2.2. *Applying differential evolution*

We already developed an analytical method [22] that determines parameters of our model. The method may find a suboptimal solution, because the model does not capture the entire system of glucose dynamics as a trade-off for the minimum required inputs (CGMS and SMBG). Therefore, we additionally applied a genetic algorithm to improve the analytically determined solution.

First, we smoothed measured IG using an approximation method [30] and determined model parameters using the original, analytical method [22]. The analytical method is based on the least squares method while applying a particular metric that determines the fitness of a given solution. Then, we proceeded with a genetic algorithm—differential evolution.

Differential evolution operates on a population of candidate solutions to a given problem. The method randomly combines, cross-breeds and mutates members of the population. Such a procedure is iteratively applied to the population, i.e., growing subsequent generations, until the best solution reaches a desired fitness. The fitness of each solution is determined using a metric. As the metric, i.e., a fitness function, we used sum of mean absolute relative error and standard deviation of relative errors of calculated BG. Relative error is absolute difference between calculated and measured BG, divided by measured BG.

The differential evolution method does not use a gradient, so the problem does not need to be differentiable. As a result, the problem can be noisy (measurement error) and change over the time (CGMS calibration).

Particularly, we used meta-differential evolution. With differential evolution, each member of the population represents one possible solution—i.e., model parameters. With meta-differential evolution, each member represents one possible solution and parameters such as mutation constant, cross rate, mutation operation, and the preferred generator of random numbers—with our implementation. The meta-differential evolution method self-tunes these parameters to optimize the possible solutions.

Nevertheless, meta-differential evolution is not guaranteed to find a solution. The first generation is generated randomly. Therefore, we set the first member of the first generation as the analytically determined solution. This way, it is guaranteed that the evolution method will not finish with a solution worse than the analytical one, while it may improve upon it.

An adverse effect of differential evolution is stagnation. With stagnation, the optimization process does not progress anymore toward finding a global optimum. Unlike premature convergence, the members remain diverse and un-converged. Typically, it occurs without any obvious reason [31]. To guarantee convergence of the method, we used different mutation strategies, which implied using two random-number generators:

1. It can be reasoned that a less uniform member selection during the mutation could avoid the stagnation. Therefore, we decided to use a deterministic chaos to generate random numbers for the current to p-best, best to bin, and current to rand1 mutation strategies. Specifically, we described the deterministic chaos with the Lyapunov exponent [31].
2. According to Zhongobo et al. [32], convergence of the differential evolution method can be proven with a uniform random number generator using a specifically designed mutation strategy. Therefore, we implemented additional strategies, using a uniform random number generator that is implemented with the Mersenne twister [33]. We added the following mutation operations: current to umpbest [32] and umbest1 [32].

Genetic algorithms mimic a natural selection of organisms. We add a local search to the differential evolution method,

Table 1 – Summarization of parsed JAEB data set.

Marker per patient	Minimum	25th percentile	Average	Median	75th percentile	Maximum
Segments	1.00	1.75	3.90	2.00	4.50	12.00
Measured BGs	31.00	36.00	45.07	42.00	51.00	82.00
Time with CGMS [hours]	24.67	83.22	109.46	121.12	142.46	143.6
Average sampling period [hours]	0.67	1.95	2.50	2.40	3.05	4.55

to mimic a human that developed a genetic engineering to alter organism's DNA so that the organism will fit better to human-designated goals in a given environment. In the implementation, we perform the local search after the selection, before evaluating the stopping condition. Local search applies local changes to a candidate solution by assuming that a better solution is close to the solution being locally modified.

As glucose levels of two compartments influence each other, we assume a possible dependency among parameters of the model. In such a case, it is not guaranteed that we will find optimal parameters only by subsequently examining global extremes by partial derivatives. With a dependency, a parameter achieves optimal value in dependency on values of one or more other parameters. We would need to re-calculate value of each parameter once another parameter value has been changed. This could lead to an indefinite cycle. With our solution, we apply the partial derivatives once and use differential evolution method to drive the changes of all parameters' values. As a result, we avoid the indefinite cycle while maintaining the diversity given by differential evolution. To calculate partial derivations numerically, we step each parameter through its discretized range while storing such a parameter value that produces the best metric value.

Differential evolution can be parallelized per population member [34–37]. In one extreme, each member is processed in a separate thread. In opposite extreme, there are several populations, called islands, each being evolved in a separate thread. The latter extreme is suited for a distributed environment. In both extremes, threads interact to share best known solutions to speed up the convergence rate of the entire evolution.

We implemented the island version, but with a parallel pipeline. Steps of the Mutation–Recombination–Selection sequence formed stages of a pipeline. Therefore, we created several populations. We repeatedly processed each population within the pipeline until we reached a stopping condition. All populations shared an extra member that held the best known global solution. On entering the pipeline, each population compared its best, population-local solution to the best global solution and updated the worse one with the better one. As a result, information about best known global solution was distributed among all populations.

With differential evolution, the domain of the p-parameter ranged from 0.0 to 2.0. The domain of the cg-parameter ranged from –0.5 to 0.0 L/mmol. The domain of the c-parameter ranged from –10.0 mmol/L to 10.0 mmol/L. The domains of the other parameters were the same as with the analytical solution [22]. Specifically, the Δt and h parameters ranged from 0 to 2400 seconds. The k-parameter ranged from –1.0 to 1.0 $s^2 \times$ L/mmol.

2.3. *Experimental setup*

The US National Institutes of Health funded Maahs et al. [38] to investigate nocturnal hypoglycemia in subjects with type 1 diabetes. This study is listed in the US Clinical Trials registry and results database under the number NCT01591681. The study evaluated a system to reduce nocturnal hypoglycemia. Study participants have had the system active in a randomized fashion. There were 45 participants using the system for 42 nights; 21 with an active system to reduce the nocturnal hypoglycemia and 21 control nights [38]. As we reached an agreement with the Jaeb Center for Health Research (JCHR), we obtained the data set of this study so that we could test our model with independently obtained data.

The data were measured using MiniMed Paradigm REALTime Veo System and Enlite glucose sensor (Medtronic Diabetes, Northridge, CA) [38]. Keenan et al. [39] examined the accuracy of the Veo system. It states that 72.92%, 26.66%, 0.54%, 3.76% and 0.12% of the measured levels fall in the A, B, C, D and E zones of the Clarke error grid, respectively. Mean absolute relative difference was 16.14% [39]; it was aggregated for all BG–IG pairs.

We parsed the original data to obtain segments of continuous measurements. For the testing, we used segments with at least 30 measured BGs so that we could design the following testing scenarios. We desired to test the model with at least 10 BGs due to the number of model parameters. Simultaneously, we were interested in testing model's accuracy if we determine its parameters with only one third of available BGs.

There were 78 segments of 20 patients, with 3516 measured BGs. Patients conducted additional SMBG measurements, which were not used to calibrate CGMS (Table 1).

To ensure robust validation of the BG calculation, we arranged the following testing scenarios:

1. We determined model parameters per each segment using all measured BGs of that segment. In addition to the differential evolution, we used this scenario with the analytical method as well to show the difference between these two methods.
2. We determined model parameters per each segment using first 20 measured BGs of that segment.
3. We determined model parameters per each segment using first 10 measured BGs of that segment.
4. We determined model parameters per each segment using every second measured BG of that segment.
5. We determined uniform model parameters for all segments using measured BGs of all segments.
6. We determined uniform model parameters for all segments using measured BGs of half of the segments.

Table 2 – Determined parameters.

Parameter		Analytical method, Scenario #1	Differential evolution scenario					
			#1	#2	#3	#4	#5	#6
p (unitless)	25th	0.955	0.965	0.929	0.890	0.974	n/a	n/a
	Med.	0.986	1.033	1.002	0.985	1.023	1.046	1.034
	75th	1.024	1.085	1.121	1.085	1.080	n/a	n/a
cg [L/mmol]	25th	–0.065	–0.043	–0.050	–0.052	–0.052	n/a	n/a
	Med.	–0.041	–0.023	–0.023	–0.031	–0.018	–0.009	–0.010
	75th	0.000	–0.003	0.000	0.000	0.000	n/a	n/a
c [mmol/L]	25th	–0.004	–0.743	–0.724	–0.755	–0.572	n/a	n/a
	Med.	0.002	–0.056	–0.008	0.004	–0.043	–0.226	–0.098
	75th	0.119	0.292	0.611	0.786	0.193	n/a	n/a
Δt [min:s]	25th	12:33	13:39	13:10	11:19	12:46	n/a	n/a
	Med.	16:11	17:03	16:47	16:50	16:59	18:52	17:57
	75th	18:39	19:09	20:59	22:17	20:27	n/a	n/a
h [min:s]	25th	00:00	00:00	00:00	00:00	00:00	n/a	n/a
	Med.	00:00	00:00	00:00	00:00	00:00	00:00	00:00
	75th	00:00	00:00	00:00	00:00	00:00	n/a	n/a
k [$s^2 \times$ L/mmol]	25th	0.000	0.000	0.000	0.000	0.000	n/a	n/a
	Med.	0.000	0.000	0.000	0.000	0.000	0.000	0.000
	75th	0.000	0.000	0.000	0.000	0.000	n/a	n/a

For Scenarios #1–#4, median (Med.) and 25th and 75th percentiles are given to illustrate shape of the distribution. On average, the *cg*-parameter was zero in approximately 21% of cases; the *k* and *h* parameters were non-zero in approximately 4% of cases. With Scenarios #5 and #6, we determined uniform model parameters for all segments. Therefore, both percentiles are not applicable to these scenarios.

With these scenarios, we satisfy the following concerns:

- While the same principles of metabolic processes apply to all subjects, the rates of the particular metabolic processes may differ for each subject. Moreover, the rates may change dynamically per segment, e.g., due to illness, drugs, physical activity, etc. Therefore, Scenarios #1–#4 calculate the parameters per each segment.
- A difference between model and parameter identification methods has to be made. Presenting a model does not preclude a development of a better method to determine model parameters. Therefore, Scenario #1 represents the so-far possible best fit that we obtained by using all measured BGs to determine the parameters.
- To verify that the model calculates missing BG properly, we have to divide the reference set of measured BGs into training set (to determine the parameters) and validation set (to validate the determined parameters). Therefore, Scenarios #2–#4 and #6 determine the parameters using various training sets.
- While the rates of metabolic processes vary per subject, they should agree on median values. Then, default model parameters should exist. Therefore, Scenarios #5 and #6 determine such parameters. Scenario #6 adds the concept of training and validation sets to this testing.

2.4. *Results*

Table 2 gives determined parameters for Scenarios #1–#6, which tested the use of differential evolution, and Scenario #1 for the analytical method.

As Equation (5) may produce such a time for which there is no measured IG, thus BG cannot be calculated at that time; Table 3 presents differences between lengths of calculated BG and measured IG. As the shortest time segment lasted 24.67 hours, the loss of approximately 20 minutes is negligible.

Table 4 gives frequency of relative error while putting it into a context with average, median and relative errors. In addition, Table 4 analyzes relative error of CGMS against measured BG. With such an analysis, we tested whether the BG calculation method would outperform CGMS in assessing BG—i.e. when considering IG as BG due to the unavailable BG measurements.

Fig. 2 depicts Table 4 by showing empirical cumulative distribution function of relative error of individual scenarios and CGMS. We sorted the relative errors in ascending order. Thus, we obtained the empirical distribution function as a step function with a stepping of $1/n$ where n is the number of calculated BG. According to the Glivenko–Cantelli theorem, such an empirical distribution function converges to the true distribution function [40,41].

Table 3 – Time periods for which BG was not calculated.

Percentile	Analytical method, Scenario #1	Differential evolution scenario					
		#1	#2	#3	#4	#5	#6
25th	12:45	13:41	12:51	11:27	13:50	18:45	17:50
Median	16:58	17:02	17:52	17:12	17:25	18:50	17:55
75th	20:24	20:14	21:43	23:35	20:49	18:50	17:55

The unit is [minute:second].

Table 4 – Frequency of relative error.

Relative error	Cumulative probability of less than or equal relative error							
	Analytical method, Scenario #1	Differential evolution scenario						CGMS' IG as BG
		#1	#2	#3	#4	#5	#6	
≤5%	29.0%	32.4%	29.5%	25.0%	30.1%	27.4%	26.8%	19.4%
≤10%	52.0%	55.4%	50.4%	45.4%	52.6%	50.2%	49.1%	37.0%
≤15%	67.8%	70.7%	66.9%	59.8%	68.3%	65.6%	64.8%	51.7%
≤20%	78.6%	81.5%	77.9%	70.7%	79.9%	77.3%	76.7%	62.8%
≤25%	85.8%	87.8%	84.6%	78.1%	86.9%	83.6%	84.2%	72.3%
≤30%	90.2%	92.1%	89.6%	83.5%	91.2%	88.5%	88.5%	79.1%
≤35%	93.2%	94.8%	92.7%	88.3%	94.4%	92.3%	92.3%	83.8%
≤40%	95.2%	96.5%	94.9%	91.3%	96.3%	94.7%	94.8%	87.1%
≤45%	96.5%	97.7%	96.1%	93.3%	97.7%	96.4%	96.6%	89.8%
≤50%	97.7%	98.1%	97.3%	94.8%	98.2%	97.2%	97.5%	91.7%
Summarization of relative errors								
Maximum	315.3%	125.7%	109.7%	308.0%	256.9%	573.1%	547.7%	269.8%
Mean	13.5%	12.2%	13.7%	16.8%	12.8%	14.3%	14.4%	21.6%
Median	9.5%	8.7%	9.9%	11.5%	9.4%	9.9%	10.2%	14.5%
Standard deviation	14.4%	12.3%	13.7%	18.2%	12.8%	17.6%	17.4%	25.3%

Each column gives probability that calculated BG has relative error less than or equal to the relative error on a respective row.

Over the years, the Clarke error grid [13,42] was accepted for determining the accuracy of CGMS with respect to the "gold-standard" of BG monitoring. The grid defines region A as those levels within 20% of the reference meter. Region B contains levels that are outside of the 20% area, but do not lead to inappropriate treatment. The other regions contain levels that would lead to unnecessary or potentially dangerous treatments (e.g., the C and D regions, respectively). Zone E identifies such levels that would confuse hypo- with hyperglycemia and vice-versa. Table 5 gives percentage of calculated BGs per zone for the analytical method and Scenarios #1–#6, which tested the use of differential evolution. In addition, it includes CGMS' IG as BG relative error.

Fig. 3 depicts an example of BG reconstruction. It supports Fig. 2 by depicting that IG and BG can differ considerably and that this will go unnoticed by CGMS. The blue curve represents CGMS-measured IG in subcutaneous tissue. Red squares represent self-monitored BG. The brown curve represents the calculated continuous BG, which fit the measured BG. In addition, Fig. 3 illustrates that the patient does no SMBG

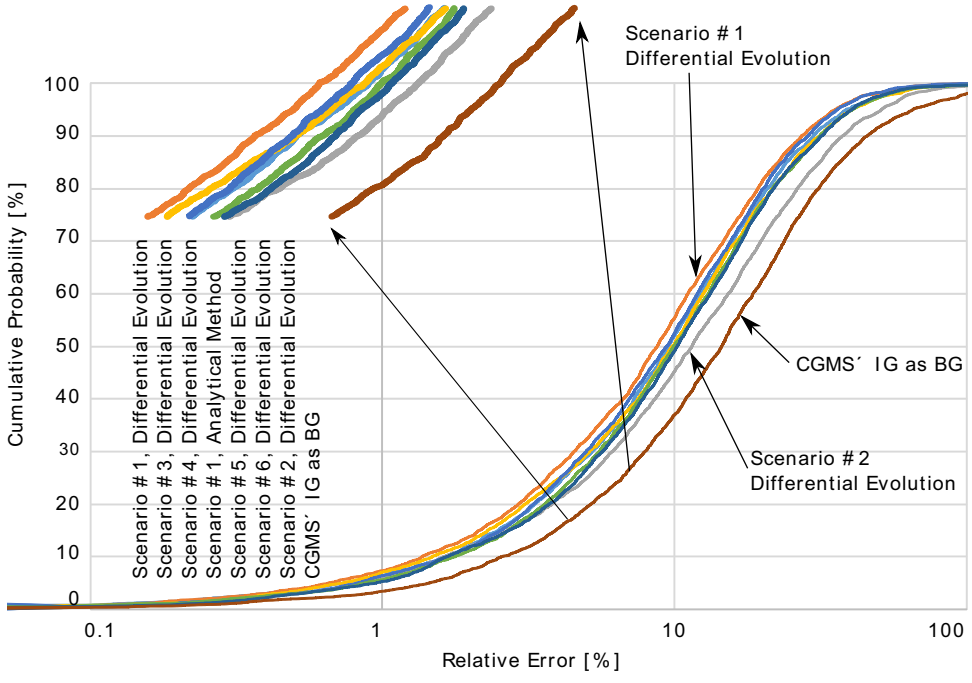

Fig. 2 – Empirical cumulative distribution function of relative error per each scenario and CGMS.

Table 5 – Clarke Error Grid analysis.

Zone	Analytical method, Scenario #1	Differential evolution scenario						CGMS' IG as BG
		#1	#2	#3	#4	#5	#6	
A	80.2%	81.5%	77.9%	70.8%	79.9%	77.3%	76.7%	65.2%
B	17.3%	15.8%	19.1%	25.9%	17.0%	19.3%	20.2%	30.4%
A+B	97.4%	97.3%	97.0%	96.7%	96.9%	96.6%	96.9%	95.6%
C	0.1%	0.1%	0.2%	0.3%	0.1%	0.4%	0.4%	0.3%
D	2.4%	2.6%	2.7%	3.0%	2.9%	3.0%	2.6%	3.9%
E	0.1%	0.0%	0.1%	0.0%	0.1%	0.0%	0.1%	0.1%

measuring in the night hours. BG and IG are not necessarily the same, and a patient has no BG for a physician to improve evaluation of that patient's night condition.

3. Discussion

This study has shown that we can successfully calculate BG with the k, h and cg parameters equal to zero. Originally, we were able to predict IG with the k and h parameters equal to zero [23] on hypertriglyceridemic rats, but with a non-zero cg-parameter. We attribute this finding to the use of the meta-differential evolution method, which identifies such a solution that cannot be determined analytically. Perhaps, the evolution algorithm adapted to the calibration procedure of CGMS. A patient may calibrate CGMS in such a manner so that IG virtually copies BG. Then, modeling the concentration gradient becomes counterproductive, because such a way of CGMS calibration erased the information needed to determine the effect of the gradient. In such a case, there is only one viable option—to calculate with zero cg-parameter.

While we were able to predict IG with zero k and h parameters, the prediction accuracy improved as we considered them as non-zero. As they are frequently zero with the Maahs et al. [38] experimental setup, there may have not been enough rapid glucose level changes to determine these parameters—contrary to a hyperglycemic clamp experimental setup [22].

Koutny [22] has demonstrated a priori determination of parameters of our model. Table 2 indicates that determined model parameters do not vary to a significant degree among the scenarios, although some variation is necessary due to the different scenario arrangements. Scenarios #1–#4 determined the parameters per segment, while Scenarios #5–#6 determined uniform parameters for all segments. For example, the c-parameter varies between Scenarios #3 and #5, but the difference is still less than the allowed 20% relative error of 4.17 mmol/L—see ISO 15197:2003 standard. This proves that model parameters can be determined using a training set of measured BG to successfully calculate BG of the validation set.

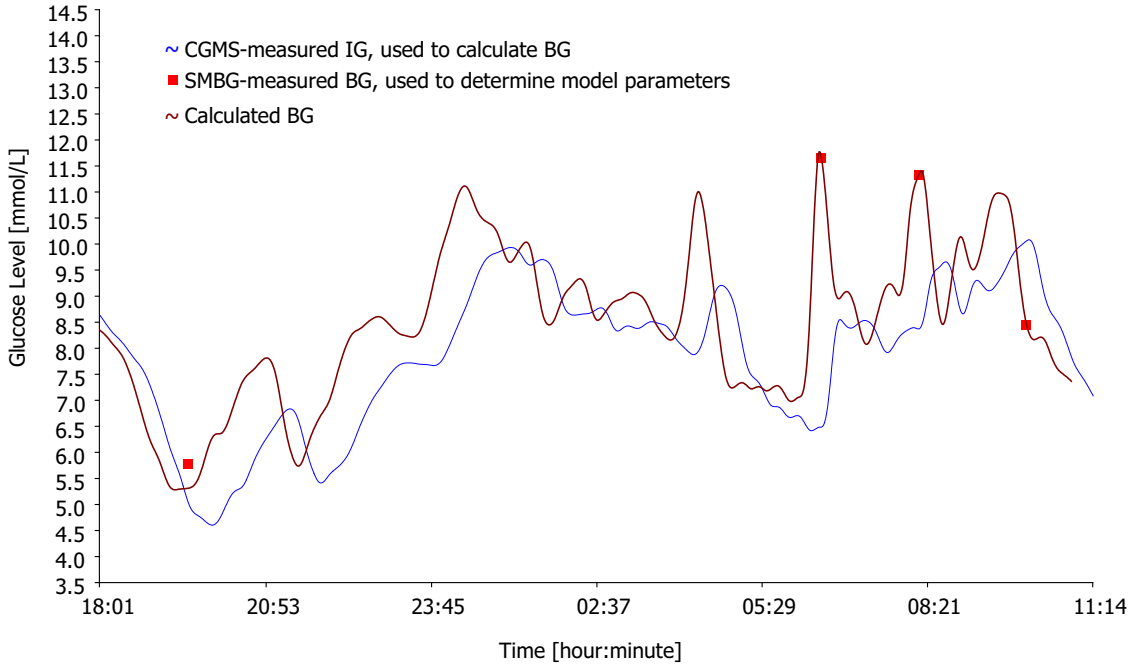

Fig. 3 – An example of BG reconstruction, Scenario #1. (For interpretation of the references to color in this figure legend, the reader is referred to the web version of this article.)

4. Conclusion

We successfully applied meta-differential evolution to make the diabetes treatment less obtrusive to the patient while giving more details to the physician. Fig. 2 depicts that any of the testing Scenarios gives more accurate estimation of BG than considering IG to be close to BG. Even Scenario #2, which used as little as 10 first BGs, performed better than CGMS in assessing BG. Scenarios #5 and #6 demonstrated that it is possible to use the model with pre-calculated parameters until enough BGs are collected to personalize the parameters.

While this paper does not update the physiological model of glucose dynamics, it is important as it verifies the entire framework (including model and parameter determination) with subjects with type 1 diabetes. Finally, we let other researchers examine our method on-line at a newly developed portal. To a diabetic patient, the portal would also serve as an educational tool to explain importance of the treatment, especially the continuous monitoring of glucose levels. The portal accepts DiaSend and Medtronic exported files. The portal's URL is https://diabetes.zcu.cz.

Acknowledgement

The Jaeb Center for Health Research (JCHR), USA provided a subset of final data from the completed, NIH-funded study entitled "Reduction of Nocturnal Hypoglycemia by Using Predictive Algorithms and Pump Suspension—an Outpatient Pilot Feasibility and Efficacy Study."

This publication was supported by the project LO1506 of the Czech Ministry of Education, Youth and Sports.

REFERENCES

[1] D. Longo, A. Fauci, D. Kasper, S. Hauser, J. Jameson, J. Loscalzo, Harrison's Principles of Internal Medicine, McGraw-Hill, New York, 2011.
[2] A.C. Guyton, J.E. Hall, Medical Textbook of Physiology, Elsevier Inc., Philadelphia, 2006.
[3] S. Vaddiraju, D. Burgess, I. Tomazos, F. Jain, F. Papadimitrakopoulos, Technologies for continuous glucose monitoring: current problems and future promises, J. Diabetes Sci. Technol. 4 (6) (2010) 1540–1562.
[4] B.W. Bequette, Continuous glucose monitoring: real-time algorithms for calibration, filtering, and alarms, J. Diabetes Sci. Technol. 4 (2) (2010) 404–418.
[5] A. Gani, A. Gribok, Y. Lu, W. Ward, R. Vigersky, J. Reifman, Universal glucose models for predicting subcutaneous glucose concentration in humans, IEEE Trans. Inf. Technol. Biomed. 14 (1) (2010) 157–165.
[6] K.L. Helton, B.D. Ratner, N.A. Wisniewski, Biomechanics of the sensor-tissue interface-effects of motion, pressure, and design on sensor performance and foreign body response—part II: examples and application, J. Diabetes Sci. Technol. 5 (2011) 647–656.
[7] S. Clarke, J. Foster, A history of blood glucose meters and their role in self-monitoring of diabetes mellitus, Br. J. Biomed. Sci. 69 (2) (2012) 83–93.
[8] K. Barnard, J. Pinsker, N. Oliver, A. Astle, E. Dassau, D. Kerr, Future artificial pancreas technology for type 1 diabetes: what do users want? Diabetes Technol. Ther. 17 (5) (2015) 311–315.
[9] A.M. Minder, A. Albrecht, J. Schafer, H. Zulewski, Frequency of blood glucose testing in well educated patients with diabetes mellitus type 1: how often is enough?, Diabetes Res. Clin. Pract. 101 (2013) 57–61.
[10] N.M. Petry, E. Cengiz, J.A. Wagner, K. Weyman, E. Tichy, W.V. Tamborlane, Testing for rewards: a pilot study to improve type 1 diabetes management in adolescents, Diabetes Care 38 (2015) 1952–1954.
[11] R.W. Beck, P. Calhoun, C. Kollman, Challenges for outpatient closed loop studies: how to assess efficacy, Diabetes Technol. Ther. 15 (2013) 1–3.
[12] L. Olansky, L. Kennedy, Finger-stick glucose monitoring: issues of accuracy and specificity, Diabetes Care 33 (2010) 948–949.
[13] S. Del Favero, A. Facchinetti, G. Sparacino, C. Cobelli, Improving accuracy and precision of glucose sensor profiles: retrospective fitting by constrained deconvolution, IEEE Trans. Biomed. Eng. 61 (4) (2014) 1044–1053.
[14] A. Haidar, M. Wilinska, J. Graveston, R. Hovorka, Stochastic virtual population of subjects with type 1 diabetes for the assessment of closed loop glucose controllers, IEEE Trans. Biomed. Eng. 60 (2013) 3254–3533.
[15] R.S. Parker, F.J. Doyle, J.H. Ward, N.A. Peppas, Robust H-infinity glucose control in diabetes using a physiological model, AIChE J. 46 (2000) 2537–2549.
[16] R. Anirban, R.S. Parker, Dynamic modeling of exercise effects on plasma glucose and insulin levels, J. Diabetes Sci. Technol. 1 (3) (2007) 338–348.
[17] C. Cobelli, C.D. Man, G. Sparacino, L. Magni, G. De Nicolao, B.P. Kovatchev, Diabetes: models, signals, and control, IEEE Rev. Biomed. Eng. 1 (2009) 54–96.
[18] V. Marmarelis, G. Mitsis, Data-Driven Modeling for Diabetes: Diagnosis and Treatment, Springer, 2014.
[19] Y. Leal, W. Garcia-Gabin, J. Bondia, E. Esteve, W. Ricart, J.-M. Fernández-Real, et al., Real-time glucose estimation algorithm for continuous glucose monitoring using autoregressive models, J. Diabetes Sci. Technol. 4 (2) (2010) 391–403.
[20] A. Facchinetti, G. Sparacino, C. Cobelli, Sensors & algorithms for continuous glucose monitoring reconstruction of glucose in plasma from interstitial fluid continuous glucose monitoring data role of sensor calibration, J. Diabetes Sci. Technol. 1 (2007) 617–623.
[21] K. Rebrin, G.M. Steil, W.P. van Antwerp, J.J. Mastrototaro, Subcutaneous glucose predicts plasma glucose independent of insulin: implications for continuous monitoring, Am. J. Physiol. 277 (1999) E561–E571.
[22] T. Koutny, Blood glucose level reconstruction as a function of transcapillary glucose transport, Comput. Biol. Med. 53 (2014) 171–178.
[23] T. Koutny, Prediction of interstitial glucose level, IEEE Trans. Inf. Technol. Biomed. 16 (2012) 136–142.
[24] T. Koutny, Glucose predictability, blood capillary permeability, and glucose utilization rate in subcutaneous, skeletal muscle, and visceral fat tissues, Comput. Biol. Med. 43 (2013) 1680–1688.
[25] T. Koutny, Estimating reaction delay for glucose level prediction, Med. Hypotheses 77 (2011) 1034–1037.
[26] D. Chen, L. Wang, J. Chen, Large-Scale Simulation: Models, Algorithms, and Applications, CRC Press, 2012.
[27] J.D. Bronzino, The Biomedical Engineering Handbook, CRC Press, Connecticut, 2006.
[28] A. Basu, S. Dube, S. Veettil, M. Slama, Y.C. Kudva, T. Peyser, et al., Time lag of glucose from intravascular to interstitial

compartment in type 1 diabetes, J. Diabetes Sci. Technol. 9 (2014) 63–68.
[29] W.K. Ward, J.M. Engle, D. Branigan, J. El Youssef, R.G. Massoud, J.R. Castle, The effect of rising vs. falling glucose level on amperometric glucose sensor lag and accuracy in Type 1 diabetes, Diabet. Med. 29 (2012) 1067–1073.
[30] T. Koutny, Modeling of compartment reaction delay and glucose travel time through interstitial fluid in reaction to a change of glucose concentration, Presented at the 10th IEEE International Conference on Information Technology and Applications in Biomedicine, Corfu, Greece, 2010.
[31] P. Kromer, I. Zelinka, V. Snasel, Can deterministic chaos improve differential evolution for the linear ordering problem? Presented at the 2014 IEEE Congress on Evolutionary Computation, Beijing, China, 2014.
[32] H. Zhongobo, X. Shengwu, S. Qinghua, Z. Xiaowei, Sufficient conditions for global convergence of differential evolution algorithm, J. Appl. Math. 2013 (2013) Article ID 193196.
[33] K. Price, R.M.L.J.A. Storn, Differential Evolution: A Practical Approach to Global Optimization, Springer, New York, 2005.
[34] R.F. Toso, M.G.C. Resende, A C++ application programming interface for biased random-key genetic algorithms, Optim. Method. Softw. 30 (2014) 81–93.
[35] S. Das, P. Suganthan, Differential evolution: a survey of the state-of-the-art, IEEE Trans. Evol. Comput. 15 (1) (2010) 4–31.
[36] R. Agrawal, A. Goyal, D. Sambasivam, A. Bhattacharya, Parallelization of industrial process control program based on the technique of differential evolution using multi-threading, in: IEEE International Conference on Industrial Engineering and Engineering Management, Bandar Sunway, Singapore, 2014.
[37] R. Lopes, R. Pedrosa Silva, A. Freitas, F. Campelo, F. Guimaraes, A study on the configuration of migratory flows in island model differential evolution, in: Conference Companion on Genetic and Evolutionary Computation Companion, Vancouver, Canada, 2014.
[38] D.M. Maahs, P. Calhoun, B.A. Buckingham, H.P. Chase, I. Hramiak, J. Lum, et al., A randomized trial of a home system to reduce nocturnal hypoglycemia in type 1 diabetes, Diabetes Care 37 (2014) 1885–1891.
[39] D.B. Keenan, R. Cartaya, J.J. Mastrototaro, Accuracy of a new real-time continuous glucose monitoring algorithm, J. Diabetes Sci. Technol. 4 (2010) 111–118.
[40] R.M. Dudley, Uniform Central Limit Theorems, Cambridge University Press, Cambridge, United Kingdom, 1999.
[41] G.R. Shorack, J.A. Wellner, Empirical Processes with Applications to Statistics, Springer-Verlag, New York, 1986.
[42] W.L. Clarke, D. Cox, L.A. Gonder-Frederick, W. Carter, S.L. Pohl, Evaluating clinical accuracy of systems for self-monitoring of blood glucose, Diabetes Care 10 (1987) 622–628.